Polarized distribution of inducible nitric oxide synthase regulates activity in intestinal epithelial cells

Martin Rumbo[1,*,†], Françoise Courjault-Gautier[2,*], Frédéric Sierro[1,‡], Jean-Claude Sirard[1,§] and Emanuela Felley-Bosco[2]

1 Swiss Experimental Cancer Research Center, Epalinges, Switzerland
2 Institute of Pharmacology and Toxicology, Lausanne, Switzerland

Correspondence

E. Felley-Bosco, Institute of Pharmacology and Toxicology, Rue du Bugnon 27, 1005 Lausanne, Switzerland
Fax: +41 21 6925355
Tel: +41 21 6925370
E-mail: emanuela.felley-bosco@unil.ch

*These authors contributed equally to the work described.

Present addresses

†Departamento de Ciencias Biológicas, Facultad de Ciencias Exactas, Universidad Nacional de La Plata, Argentina
‡The Garvan Institute of Medical Research, Darlinghurst, Australia
§Institut de Biologie de Lille, Groupe AVENIR, Equipe Mixte INSERM, Université E0364, Lille, France

Inducible nitric oxide synthase (iNOS) functions as a homodimer. In cell extracts, iNOS molecules partition both in cytosolic and particulate fractions, indicating that iNOS exists as soluble and membrane associated forms. In this study, iNOS features were investigated in human intestinal epithelial cells stimulated with cytokines and in duodenum from mice exposed to flagellin. Our experiments indicate that iNOS is mainly associated with the particulate fraction of cell extracts. Confocal microscopy showed a preferential localization of iNOS at the apical pole of intestinal epithelial cells. In particulate fractions, iNOS dimers were more abundant than in the cytosolic fraction. Similar observations were seen in mouse duodenum samples. These results suggest that, in epithelial cells, iNOS activity is regulated by localization-dependent processes.

The inducible nitric oxide synthase (iNOS) protein is responsible for sustained release of nitric oxide (NO) and is typically synthesized in response to proinflammatory stimuli [1]. iNOS protein is induced in a large variety of human diseases, including intestinal disorders such as chronic inflammatory bowel diseases and colon adenocarcinoma [2–4]. The pathobiological function of NO still remains largely uncertain in view of the multiple and even opposite effects of NO. In fact, besides the amount of NO produced, it has been recently suggested that the NO-mediated actions depend on many other factors such as the nature of iNOS induction signal, the cellular and subcellular site of production, subsequent interactions with other cell components and the redox environment [5–7]. Although iNOS was originally described as a cytosolic

Abbreviations
DOC, sodium deoxycholate; iNOS, inducible nitric oxide synthase; NO, nitric oxide; TX-100, Triton X-100.

protein [8], it is distributed between the cytosol and particulate fraction in activated macrophages [9–11]. It is also present in the particulate but not the cytosolic fraction from guinea pig skeletal muscle [12] and it localizes *in vivo* to the apical domain of human bronchial and kidney epithelial cells [13]. iNOS protein is active in a dimeric form [14] but both dimers and monomers can be found in the cytoplasm. About 60% of cytosolic iNOS are dimeric in activated murine macrophages [15] and 70% in activated rat hepatocytes [16]. However, nothing is known about the dimer/monomer ratio of particulate iNOS. This may be relevant for understanding the control of iNOS and defining targeting strategies for iNOS inhibition. The aim of this study was therefore to characterize iNOS activity both *in vitro*, using cytosolic and particulate fraction of activated human intestinal epithelial cells [17], and *in vivo*, using duodenum samples from mice exposed to bacterial flagellin, which is known to up-regulate iNOS expression in intestinal epithelial cells [18].

Results

Subcellular distribution of iNOS protein and activity *in vitro*

The distribution of iNOS protein in the cytosol and particulate fraction was examined in DLD-1 cells exposed to cytokines. To determine the partitioning of iNOS into soluble cytosolic and insoluble membrane-associated forms, cell fractionation was performed. As expected, lactate dehydrogenase activity was recovered at $98 \pm 4\%$ ($n = 4$) in the cytosolic fraction, while membrane protein Na^+/K^+-ATPase was detected only in the particulate fraction (Fig. 1A), indicating that the fractionation procedure is effective. iNOS protein was distributed at $66 \pm 2\%$ and $34 \pm 2\%$ in the particulate fraction and cytosol, respectively (Fig. 1B,C), leading to a particulate to cytosol ratio of 2.0 ± 0.1. To investigate whether iNOS was delivered as an active enzyme, citrulline production was also determined. Interestingly, compared to the iNOS protein ratio, iNOS activity partitioned in higher proportion in particulate vs. cytosolic fraction ($66 \pm 2\%$ vs. $19 \pm 1\%$, respectively) (Fig. 1D). In conclusion, iNOS specific activity was 1.8 ± 0.1-fold higher for particulate-bound iNOS than for the cytosolic one ($P < 0.001$).

Subcellular distribution of iNOS dimers and monomers

To further characterize iNOS activity, various solubilization protocols as described below were applied to
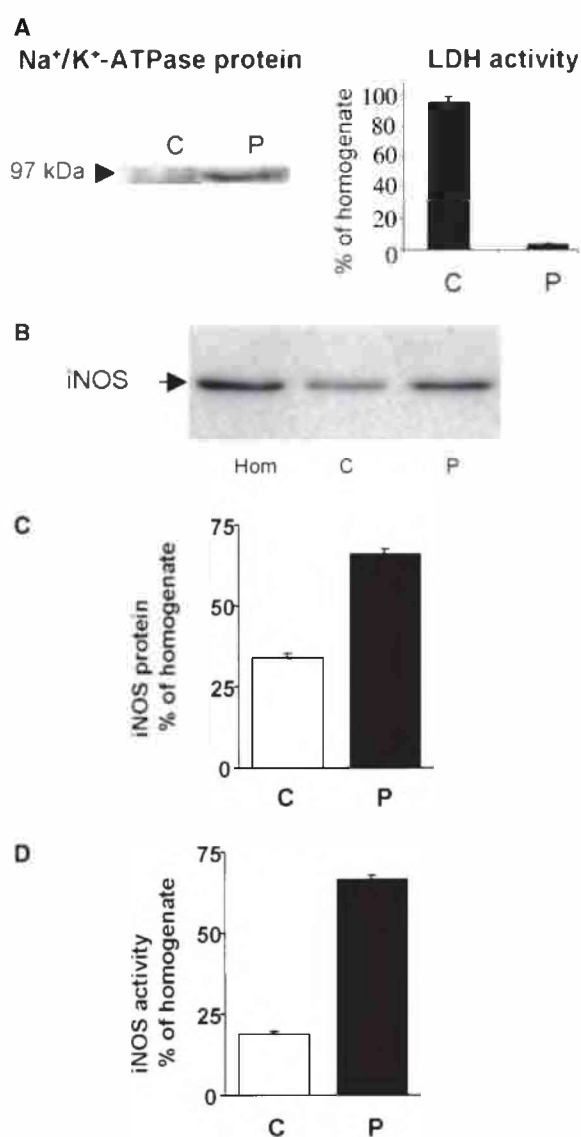

Fig. 1. Subcellular distribution of iNOS in human cultured intestinal cells. DLD-1 cells were incubated with cytokines for 14 h before cell fractionation. (A) Distribution of Na^+/K^+-ATPase or LDH in cytosol (C) and particulate (P) fractions. (B) Subcellular distribution of iNOS protein. Equal volumes of the cytosolic and particulate were analyzed. (C) Densitometric analysis of iNOS protein distribution. The protein amount in each fraction was expressed relative to the iNOS amount found in homogenate and values are the means ± SEM from seven independent experiments. (D) Subcellular distribution of iNOS activity. The enzyme activity was determined by the amount of citrulline produced in cytosol vs. resuspended particulate fraction and was expressed as percentage of the production measured in the whole cell homogenate (64.3 ± 6.3 pmol·min^{-1}·mg protein^{-1} $n = 7$). Values are the means ± SEM from seven independent experiments.

particulate fractions. As shown in Fig. 2A, complete iNOS protein solubilization was achieved by Triton X-100 (TX-100)/NaCl or Lubrol/sodium deoxycholate
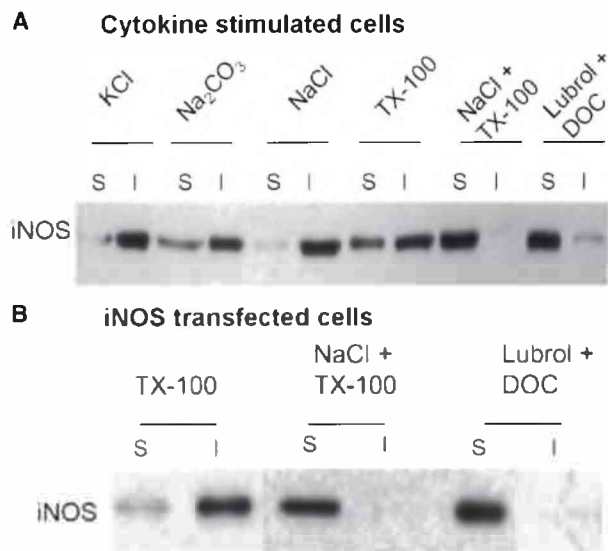
A **Cytokine stimulated cells**

B **iNOS transfected cells**

Fig. 2. Effect of salts and detergents on iNOS association with membranes in cultured cells. (A) Particulate fractions prepared from cytokine-treated cells were extracted with 1 M KCl or incubated for 1 h with one of the following components prepared in lysis buffer: 0.1 M Na_2CO_3 pH 11; 125 mM NaCl; 1% TX-100; 1% TX-100 together with 125 mM NaCl; or sonicated after addition of Lubrol/DOC. Soluble (S) and insoluble (I) material were separated by centrifugation at 100 000 *g*. The insoluble pellet was resuspended by sonication in the same volume as supernatant and equal volumes of the two fractions were loaded. (B) Particulate fractions prepared from DLD-1 cells transfected with iNOS were incubated for 1 h with one of the following components prepared in lysis buffer: 1% TX-100; 1% TX-100 together with 125 mM NaCl; or sonicated after addition of Lubrol/DOC. Soluble (S) and insoluble material (I) were separated by centrifugation at 100 000 *g*. The insoluble pellet was resuspended by sonication in the same volume as supernatant and equal volumes of the two fractions were loaded. Blots shown are representative of three independent experiments.

(DOC). However, TX-100/NaCl reduced iNOS activity by 51 ± 2% (*n* = 3). Solubilization with Lubrol/DOC was highly effective compared to other methods and resulted in recovery of most iNOS activity (91 ± 6%) indicating that this method is more appropriate to solubilize functional iNOS.

In order to determine the influence of cytokine signaling on biochemical properties of iNOS, DLD-1 cells transfected with iNOS were investigated. As in cytokine-stimulated cells, complete iNOS solubilization from the particulate fraction was obtained with TX-100/NaCl or Lubrol/DOC (Fig. 2B). In transfected cells it was also possible to verify that the same activity was recovered when cells were harvested either in lysis buffer or in Lubrol/DOC (data not shown), indicating that treatment with these detergents does not result in artificial increase of iNOS activity.
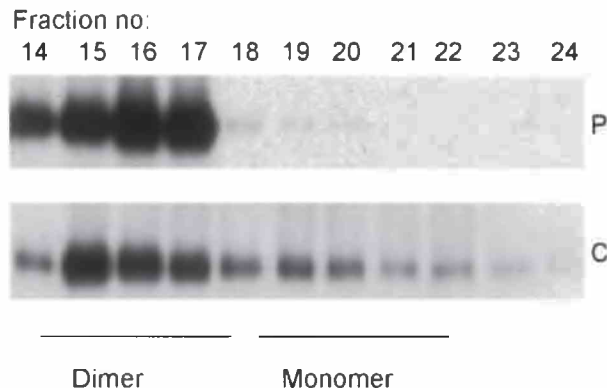

Fig. 3. Distribution of iNOS monomers and dimers in solubilized particulate fraction (P) and cytosol (C) of DLD-1 cells stimulated for 14 h with cytokines. Lubrol/DOC extracts of particulate fraction and cytosols were fractionated by gel filtration chromatography and column fractions were analyzed by SDS/PAGE and Western blot. Fractions were designated to contain iNOS dimers or monomers based on the estimated molecular mass of the gel filtration fraction. Blot shown is representative of three independent experiments.

Taken together these data indicate that in epithelial intestinal cells iNOS intrinsically associates with particulate matter and intact activity can be extracted with Lubrol/DOC.

Because iNOS activity requires dimerization [14], we investigated iNOS oligomerization in cell fractions using gel filtration chromatography, which allows definition of the amount of monomers and dimers. Western blot analysis of chromatography fractions showed that only dimers were present in the particulate compartment (Fig. 3). In contrast, some cytosolic iNOS is in monomeric form (monomers/dimers estimated to 0.33 ± 0.06, *n* = 3). Using this information it is possible to calculate how much of the protein present in the cytosol (34% of total iNOS, Fig. 1C) is in the dimeric form. Indeed total protein in this compartment is represented by the sum of monomer plus dimer. Knowing that monomer = 0.33 × dimer, total iNOS protein is equivalent to 1.33 × dimer. Therefore, the amount of total cellular dimer that is cytosolic dimer was estimated to 26% (34%/1.33). Thus, iNOS specific activity standardized to iNOS dimer levels was not significantly different in particulate-associated and cytosolic iNOS. In conclusion, these results suggest that the prevalence of iNOS dimers is essential for enrichment in iNOS activity within the particulate fraction of epithelial cells.

Apical distribution of iNOS in intestinal epithelial cells

To get more insight into the localization of iNOS in intestinal cells, Caco-2 cells were investigated. Caco-2

cells spontaneously differentiate to enterocyte-like cells when they are cultured for 20 days after confluence onto plastic or for 10 days on filters. At this stage they form polarized monolayers sealed by tight junctions, and display a well-developed apical brush border membrane expressing specific enterocyte hydrolases [19]. As described previously [20], iNOS protein decreased upon differentiation in Caco-2 cells (Fig. 4A, left). After cytokine addition, iNOS expression was dramatically increased in Caco-2 cells in both proliferating and differentiated cells (Fig. 4A, left). iNOS was also expressed after Caco-2 transfection with human iNOS cDNA (Fig. 4A, right). As in DLD-1 cells, iNOS was mainly associated to particulate matter in cytokine-activated or iNOS-transfected cells (data not shown). To correlate the iNOS partitioning in the particulate fraction to a specific subcellular distribution, immunostaining was performed on differentiated enterocytes
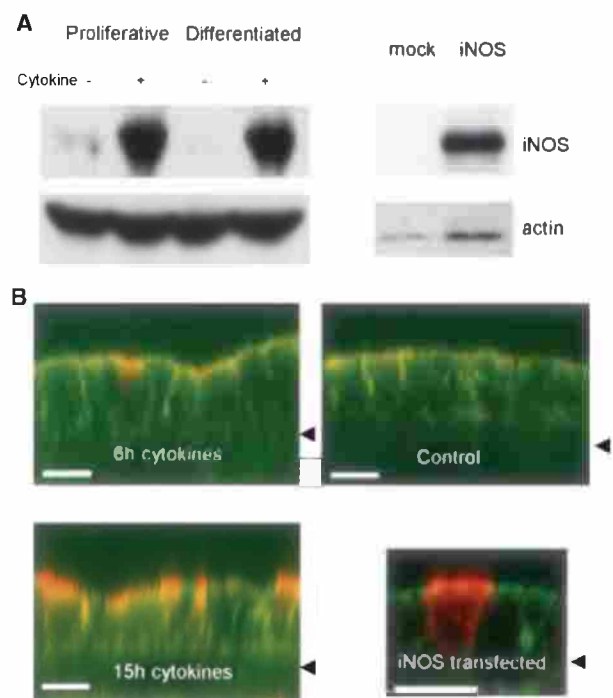
(Fig. 4B). Confocal microscopy showed that iNOS localized to the apical domain of enterocytes and colocalized with filamentous actin (Fig. 4B, left). The apical distribution was independent of cytokine stimulation as assessed with Caco-2 cells transfected with human iNOS cDNA (Fig. 4B, bottom right).

Taken together, these data suggest a specific localization of iNOS to apical domains of intestinal epithelial cells.

Particulate fraction association of iNOS *in vivo*

In order to determine the distribution of iNOS in intestinal epithelial cells *in vivo*, experiments were conducted in mice injected with bacterial flagellin. Flagellin activates Toll-like receptor 5, which induces iNOS expression in intestinal epithelial cells *in vivo* [18]. Quantitative RT-PCR showed five-fold induction of iNOS mRNA levels in the duodenum of flagellin-treated compared to untreated animals (Fig. 5A). We also found a 50-fold induction of iNOS mRNA levels in microdissected epithelium from villi (Fig. 5A), which indicates that epithelial cells were the main source of iNOS. In addition, production of iNOS protein was significantly up-regulated in mice exposed to flagellin (Fig. 5B). Immunostaining of duodenum sections revealed that iNOS was distributed apically in
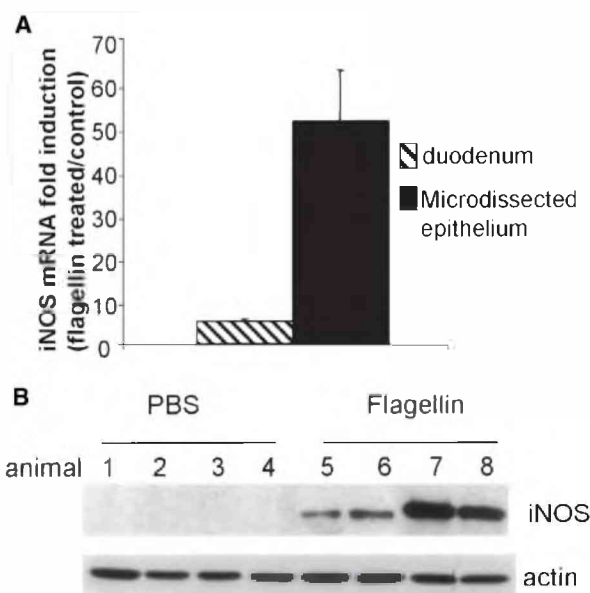

Fig. 4. iNOS localizes to the apical domain of polarized intestinal epithelial cells. (A) Western blot analysis of iNOS expression 15 h after cytokine stimulation of proliferative vs. differentiated cells (left) or in Caco-2 cells transfected with iNOS (right). Actin was used as control for protein loading. (B) XZ confocal sections of cytokine treated Caco-2 cells (left) or iNOS transfected Caco-2 cells (bottom right, not all transfected cells expressed iNOS). Cells were immunostained using anti-iNOS and phalloidine (F-actin detection). Only F-actin staining was observed when sections from cells exposed to cytokine for 15 h were stained without the iNOS primary antibody (control: upper right). The arrows indicate the position of the filter (basolateral side of cells). Scale bar = 6 μm.

Fig. 5. Expression of iNOS in duodenum tissue of mice. (A) Quantification of iNOS mRNA induction by flagellin in whole tissue and microdissected epithelium from villi assessed by real-time PCR. (B) Western blot analysis of iNOS protein expression in control or flagellin-exposed mice. Actin was used as control for protein loading.
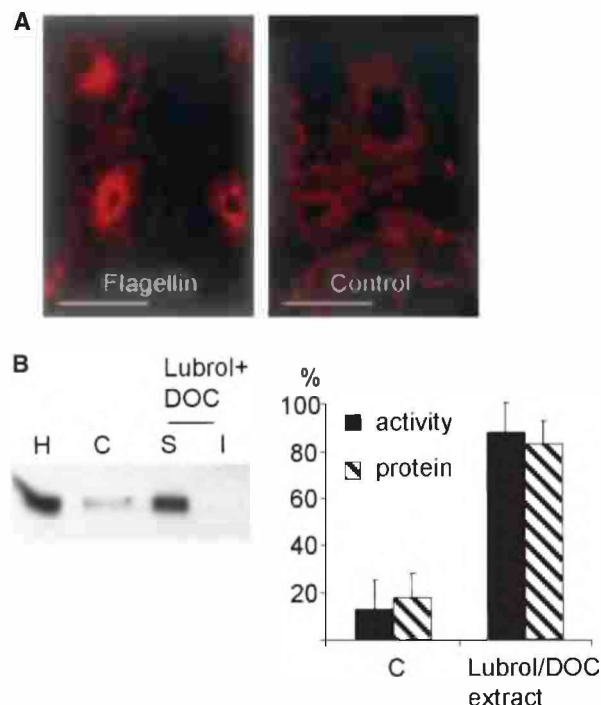
Fig. 6. Subcellular distribution of iNOS in murine duodenum tissue. (A) Duodenum sections of flagellin-exposed or control mice were immunostained using anti-iNOS IgG. Each condition is representative of three mice. Scale bar = 40 μm. (B) Homogenate (H), cytosolic (C), Lubrol/DOC-extracted particulate fractions (S) and insoluble pellet (I) were analyzed by Western blot (left). Densitometric analysis of iNOS protein and distribution of iNOS activity in cytosol vs. Lubrol/DOC extracts (right). Whole duodenum homogenate activity amounted to 32 ± 14 pmol citrulline·min^{-1}·mg $protein^{-1}$ ($n = 4$). Values are the means ± SEM from four independent experiments.

intestinal crypts (Fig. 6A) corroborating the observation in cultured polarized cells. Soluble and particulate fractions were extracted from intestinal homogenate from flagellin exposed mice and analyzed by Western blot (Fig. 6B, left). We found that iNOS protein was 4.6-fold more abundant in the particulate fraction than in the cytosol ($82 \pm 10\%$ vs. $18 \pm 10\%$, respectively). iNOS activity was distributed $87 \pm 12\%$ in the particulate fraction and $13 \pm 12\%$ in the cytosolic fraction (Fig. 6B, right). Thus, iNOS activity normalized by total iNOS protein was 1.5-fold higher for particulate-bound iNOS than for the cytosolic ($P < 0.05$).

The iNOS monomer/dimer ratio was 0.60 ± 0.08 ($n = 3$) for the cytosolic fraction and 0.20 ± 0.04 ($n = 3$) for the particulate fraction. Using the same calculation as for cultured cells, the amount of total dimer that is cytosolic or particulate dimer was estimated to 11% (18%/1.6) and 69% (82%/1.2), respectively. Therefore, the preferential partitioning of iNOS

activity into the particulate fraction probably results from the enrichment in iNOS dimers.

Discussion

While the occurrence of iNOS in the particulate cellular fraction has been known for several years [9–11,13], the biological significance of this association is not clear at the moment. Our results showed that both *in vitro* and *in vivo*, most iNOS protein or activity is associated with the particulate fraction in intestinal epithelial cells. These results are consistent with iNOS features in neutrophils from the urine of patients with bacterial urinary tract infection [21], primary proximal tubules, human bronchial epithelial cells 16HBE1-4o- [13] and activated rodent macrophages [9–11,22]. Previous studies have shown that iNOS interacts with cytoskeleton via components like α-actinin 4 [22] and other proteins harboring a spectrin-like motif [23]. We found that epithelial iNOS also colocalized with actin cytoskeleton proteins on the apical side of polarized intestinal cells. A recent study shows that the C-terminus of iNOS promotes *in vitro* interactions with the PDZ protein EBP50 [13]. Interestingly, EBP50 has different binding partners including ezrin that can be anchored to the actin cytoskeleton [24]. The potential contribution of ezrin in apical distribution of iNOS is inferred from the observation that ezrin is concentrated beneath the plasma membrane in apical microvilli in the epithelium of the small intestine [25].

Our solubilization protocol allows efficient recovery of iNOS activity and analysis of the monomer/dimer ratio in particulate fractions [14–16,26]. Previous investigations focused on cytosolic fractions or fractions soluble in 0.1% (v/v) TX-100 [22], which do not represent total iNOS [10]. Our data show that iNOS activity in epithelial cells is not only controlled by the number of iNOS molecules but also by the oligomerization feature in subcellular fractions. Previous studies have shown variation in iNOS specific activity in correlation to subcellular localization. Indeed, in murine macrophages stimulated by lipopolysaccharide, iNOS binds Rac2, a member of the Rho GTPase family, and overexpression of Rac2 leads to a specific distribution of iNOS to the insoluble fraction. This effect is accompanied by increased iNOS activity without any change in iNOS protein levels [27]. Although the molecular mechanisms of Rac2-dependent regulation of iNOS activity are not elucidated yet, these data indicate compartmentalization-mediated regulation. In another study [22], disruption of iNOS interaction with cytoskeletal protein α-actinin 4 resulted in iNOS redistribution and loss of activity.

Targeting iNOS activity to specific cellular domains is independent of stimulation as a similar distribution is observed in transfected cells. Taken together these observations indicate that cells set up efficient strategies to bring iNOS to where NO production is required. This may be necessary, as proposed by others [28], to direct NO toward extracellular pathogens, which, in intestinal cells, could be bacteria present in the intestinal lumen. This hypothesis is supported by positioning of iNOS on the apical side of intestinal crypts. Recently PDZ-binding α_2/β_1-NO-sensitive guanylate cyclase [29] was also found expressed in intestinal tissue [30]. Active iNOS might be targeted to this NO-sensitive form of guanylate cyclase via association with a PDZ protein anchoring both NO-sensitive guanylate cyclase and iNOS. NO can also interact with superoxide to form the strong oxidant peroxynitrite [31,32]. Superoxide is produced *in vivo* by membrane-associated NADPH oxidase complex, which is present in intestinal epithelial cells [33–35]. Exposure of NADPH oxidase expressing-human intestinal cells to flagellin can increase superoxide production [35]. Combined with our observation that flagellin increases expression of a particulate fraction-associated iNOS, this suggests a colocalization and a functional interaction between these enzymes.

Different scenarios can be considered according to the iNOS dimer enrichment in the particulate fraction. One possibility is that the scaffolding protein anchoring iNOS to the particulate fraction recognizes mainly the active dimer. This might explain why under denaturing conditions iNOS did not immunoprecipitate with PDZ protein EBP50 [13]. Alternatively, monomers might have distinct turnover rates depending on their subcellular localization. The fact that the antifungal molecule clotrimazole is able to change the ratio of dimeric to monomeric iNOS in the cytosol without affecting total protein amount [26,36] favors the hypothesis that iNOS monomers are stable in the cytosol. On the other hand we have shown that proteasomal iNOS degradation seems to occur in detergent insoluble domains [17].

In conclusion, this study in cytokine- or flagellin-stimulated intestinal epithelial cells corroborated previous observations of iNOS accumulation in the particulate cellular fraction and showed for the first time that the monomeric to dimeric iNOS ratio is different in particulate vs. cytosolic fractions. These results indicate a new regulation of iNOS activity relying on localization-dependent molecular conformation and provide tools for further investigation of the mechanisms involved in this differential iNOS distribution.

Experimental procedures

Cell culture

Human intestinal epithelial DLD-1 cells (ATCC CCL-221) were cultured and stimulated with 100 U·mL^{-1} interferon-γ, 200 U·mL^{-1} interleukin-6 (Roche Molecular Biochemicals, Rotkreuz, Switzerland), and 0.5 ng·mL^{-1} interleukin-1β (Calbiochem, La Jolla, CA, USA) to induce iNOS as described previously [17]. A stimulation period of 14 h was selected from a time course study establishing that iNOS production and activity, which were undetected in control cells, reached maximal levels within 10 h of cytokine exposure and then remained stable during the following 6 h [37].

To investigate iNOS induction in polarized epithelial cells, human intestinal epithelial Caco-2 clone 1 cells, stimulated with cytokines as above were used. Caco-2 cells were grown either on plastic dishes as described previously [20], or on Transwell (6 mm in diameter, 3 µm pore; Corning Costar, Cambridge, MA, USA) where integrity of the epithelial layer was verified by measurement of transepithelial resistance [38].

In some experiments DLD-1 or Caco-2 cells transfected with human iNOS coding cDNA [39] subcloned into the *Not*I site of the pCIpuro vector, which contains a puromycin resistance gene (kindly provided by J Mirkovitch, Swiss Institute for Experimental Cancer Research, Epalinges, Switzerland) were used.

Mice exposure to flagellin

Protocols involving animals were reviewed and approved by the State Authority (Commission du Service Veterinaire Cantonal, Lausanne, Switzerland). C57BL/6 mice (8–10 weeks old) were challenged (intravenously) with 1 µg of flagellin purified as described previously [38]. Mice were killed after 2 h by cervical dislocation and duodenal tissue was processed for RNA and protein analysis as described below.

Cell or tissue lysate preparation and subcellular fractionation

Cell monolayers or 1 cm duodenum tissue were suspended in lysis buffer (50 mM Hepes pH 7.4, 1 mM EGTA, 10% glycerol, 2 µM tetrahydrobiopterin, 2 µM FAD, 5 µg·mL^{-1} pepstatin, 3 µg·mL^{-1} aprotinin, 10 µg·mL^{-1} leupeptin, 0.1 mM 4-(2-aminoethyl)-benzenesulfonyl fluoride, 1 mM sodium vanadate and 50 mM sodium fluoride). Cell samples were then homogenized by three freeze/thaw cycles. Tissues were homogenized using Polytron (Kinematica AG, Littau, Switzerland). Aliquots of homogenate were centrifuged at 100 000 g for 15 min at 4 °C (Beckman Optima TLX Ultracentrifuge, Nyon, Switzerland). The pellet corresponding to the particulate fraction (48.4 ± 2.7% and 53.8 ± 4.7% of

the protein in cultured cells and tissue, respectively) was re-suspended by two freeze/thaw cycles in a final volume of lysis buffer equal to the cytosolic volume. To check cell fractionation, activity of the cytosolic marker lactate dehydrogenase was measured [40] and Western blot analysis of Na^+/K^+-ATPase, a membrane marker, was performed using an antibody raised against rabbit α-subunit (1 : 20 000) [41].

To further characterize epithelial iNOS, the particulate fraction, was exposed to one of the following treatments: (a) extraction with 1 M KCl; (b) incubation for 1 h at 4 °C with one of the following components prepared in lysis buffer: 0.1 M Na_2CO_3 pH 11; 125 mM NaCl; 1% (v/v) TX-100; 1% (v/v) TX-100 in the presence of 125 mM NaCl; (c) resuspension in 0.17 M sucrose, 30% (v/v) glycerol, 10 mM glycine buffer, pH 8.0, containing 0.25% (v/v) each of DOC and Lubrol PX and 1.6 μM $CaCl_2$ and immediate sonication at full power for 10 s at 4 °C [42]. All extracts were separated by centrifugation at 100 000 *g*. The supernatant, corresponding to the soluble fraction, was retained and the resulting pellet, corresponding to insoluble material, was resuspended by sonication in the same volume as supernatant.

iNOS activity

Calcium-independent NOS activity was assessed by measuring the conversion of L-[H³]arginine to L-[H³]citrulline, as described previously [43]. iNOS specific activity was calculated from the ratio of citrulline production to iNOS protein levels.

Western blot analysis

Proteins determination and Western blot analysis were performed as described previously [17,20]. Denatured proteins were separated on 7.5% SDS/polyacrylamide gel. Antibody raised against human iNOS (kind gift of RA Mumford, Merck Research Laboratories, Rahway, NJ, USA), or murine iNOS (Transduction Laboratories, Lexington, KY, USA) were diluted at 1 : 40 000 or 1: 2 000, respectively. Detection was achieved by enhanced chemiluminescence (Amersham Pharmacia, Dubendorf, Switzerland) and densitometry (Imagequant, Amersham Bioscience, Uppsala, Sweden) was performed on nonsaturated films. An internal calibration curve, obtained with increasing amounts of homogenate, allowed the determination of the linearity conditions of the luminescence reaction.

Laser dissection microscopy, RNA isolation and real-time PCR

The gut was rinsed with ice-chilled $NaCl/P_i$ to remove the intestinal content. One centimeter long duodenum segments were cut and villi epithelium was microdissected to extract RNA and prepare cDNA as described previously [44]. The latter was amplified by the SYBR-Green real-time PCR assay, and products were detected on a Prism 5700 detection system (ABI/PerkinElmer, Foster City, CA, USA). Beta actin RNA was used to standardize the total amount of cDNA. Primers for iNOS (GCTGCCAGGGTCACAAC TTT and ACCAGTGACACTGTGTCCCGT) and for beta actin (GCTTCTTTGCAGCTCCTTCGT and CGTCATCC ATGGCGAACTG) yielded PCR products of 71 and 59 bp, respectively. Specificity of PCR was checked by analyzing the melting curve. Relative mRNA levels were determined by comparing (a) the PCR cycle threshold between cDNA of iNOS and beta actin (ΔC), and (b) ΔC values between treated and untreated conditions (ΔΔC) as described previously [7,44].

Immunostaining and confocal microscopy

Caco-2 cells grown on Transwell filters were fixed with $NaCl/P_i$ 4% (v/v) paraformaldehyde then permeabilized for 5 min with $NaCl/P_i$ 1% (v/v) TX-100. Immunostaining was carried out by incubation with NO53 anti-iNOS IgG 1 : 10 000 followed by detection using Cy3-conjugated anti-rabbit IgG (Jackson Immunoresearch Laboratories, West Grove, PA, USA) at a dilution of 1 : 200 for 45 min. Filamentous actin expression was detected with Alexa Fluor 488 phalloidin (Molecular Probes, Inc., Eugene, OR, USA). Caco-2 monolayers were analyzed by an LSM-410 Zeiss confocal microscope (Feldbach, Switzerland). XZ sections of monolayers were performed to determine iNOS localization.

Tissue specimens were frozen in OCT embedding compound (Sakura Finetek Europe, Zoeterwoude, the Netherlands) and stored at −80 °C. Sections (5 μm thick) were fixed with $NaCl/P_i$ 4% (v/v) paraformaldehyde then immersed in 0.01 M sodium citrate buffer (pH 6.0) and placed into a microwave oven for 10 min before incubation with the primary antiserum. Antigen retrieval treatment significantly reduced the strong background obtained in tissue using anti-murine iNOS IgG. Sections were permeabilized for 5 min with $NaCl/P_i$ 0.2% (v/v) TX-100, then sequentially incubated with $NaCl/P_i$ containing 2% (w/v) BSA, anti-murine iNOS (overnight at 4 °C), followed by detection using Cy3-conjugated anti-rabbit IgG. Because microwave treatment abolishes phalloidin immunoreactivity, phalloidin staining was not performed on tissue sections. For control of unspecific binding of the antibodies, we performed control incubations by applications of isotype matched antibodies directed against different defined antigens. All control experiments were negative. Immunofluorescence was observed with a Zeiss Axiophot immunofluorescence microscope.

Gel filtration chromatography

To determine the relative amounts of iNOS dimers and monomers present in cytosolic and solubilized particulate

fractions, size exclusion chromatography was carried out at 4 °C using a Sephadex G200 gel filtration column as already described for cytosolic fractions [15,16] or fractions soluble in TX-100 [22]. The column was equilibrated with 40 mM Bistris buffer pH 7.4, containing 2 mM dithiothreitol, 10% (v/v) glycerol and 100 mM NaCl for human iNOS or 200 mM NaCl for murine iNOS [15,16]. Fractions were analyzed for iNOS protein by Western blot. The molecular masses of the protein fractions were estimated relative to gel filtration molecular mass standards. Gel filtration fractions that fell within a molecular mass range of 600–50 kDa (14 fractions) were analyzed by Western blot as described above. The intensity of the iNOS bands was quantitated by densitometry, integrated, and the ratio between monomers and dimers was calculated from these values.

Data analysis

Values are means $\pm$ SEM of n independent experiments and statistical analysis was performed using Student's t-test.

Acknowledgements

References

1 MacMicking J, Xie QW & Nathan C (1997) Nitric oxide and macrophage function. *Annu Rev Immunol* **15**, 323–350.

2 Kroncke KD, Fehsel K & Kolb-Bachofen V (1998) Inducible nitric oxide synthase in human diseases. *Clin Exp Immunol* **113**, 147–156.

3 Ambs S, Merriam WG, Bennett WP, Felley-Bosco E, Ogunfusika MO, Oser SM, Klein S, Shields PG, Billiar TR & Harris CC (1998) Frequent nitric oxide synthase-2 expression in human colon adenomas: implication for tumor angiogenesis and colon cancer progression. *Cancer Res* **58**, 334–341.

4 Singer II, Kawka DW, Scott S, Weidner JR, Mumford RA, Riehl TE & Stenson WF (1996) Expression of inducible nitric oxide synthase and nitrotyrosine in colonic epithelium in inflammatory bowel disease. *Gastroenterology* **111**, 871–885.

5 Espey MG, Miranda KM, Pluta RM & Wink DA (2000) Nitrosative capacity of macrophages is dependent on nitric-oxide synthase induction signals. *J Biol Chem* **275**, 11341–11347.

6 Miller MJS & Sandoval M (1999) Nitric Oxide III. A molecular prelude to intestinal inflammation. *Am J Physiol* **276**, G795–G799.

7 Andre M & Felley-Bosco E (2003) Heme oxygenase-1 induction by endogenous nitric oxide: influence of intracellular glutathione. *FEBS Lett* **546**, 223–227.

8 Moncada S, Palmer RMJ & Higgs EA (1991) Nitric oxide: physiology, pathophysiology, and pharmacology. *Pharmacol Rev* **43**, 109–142.

9 Schmidt HHHW, Warner TD, Nakane M, Fostermann U & Murad F (1992) Regulation and subcellular location of nitrogen oxide synthases in RAW264.7 macrophages. *Mol Pharmacol* **41**, 615–624.

10 Vodovotz Y, Russell D, Xie Q, Bogdan C & Nathan C (1995) Vesicle membrane association of nitric oxide synthase in primary mouse macrophages. *J Immunol* **154**, 2914–2925.

11 Webb JL, Harvey MW, Holden DW & Evans TJ (2001) Macrophage nitric oxide synthase associates with cortical actin but is not recruited to phagosomes. *Infect Immun* **69**, 6391–6400.

12 Gath I, Closs EI, Gödtel-Armbrust U, Smitt S, Nakane M, Wessler I & Förstermann U (1996) Inducible NO synthase II and neuronal NO synthase I are constitutively expressed in different structures of guinea pig skeletal muscle: implications for contractile function. *FASEB J* **10**, 1614–1620.

13 Glynne PA, Darling KE, Picot J & Evans TJ (2002) Epithelial inducible nitric oxide synthase is an apical EBP50-binding protein that directs vectorial nitric oxide output. *J Biol Chem* **277**, 33132–33138.

14 Baek KJ, Thiel BA, Lucas S & Stuehr DJ (1993) Macrophage Nitric Oxide Synthase Subunits. *J Biol Chem* **268**, 21120–21129.

15 Albakri QA & Stuehr DJ (1996) Intracellular assembly of inducible NO synthase is limited by nitric oxide-mediated changes in heme insertion and availability. *J Biol Chem* **271**, 5414–5421.

16 Park JH, Na HJ, Kwon YG, Ha KS, Lee SJ, Kim CK, Lee KS, Yoneyama T, Hatakeyama K, Kim PK, Billiar TR & Kim YM (2002) Nitric oxide (NO) pretreatment increases cytokine-induced NO production in cultured rat hepatocytes by suppressing GTP cyclohydrolase I feedback inhibitory protein level and promoting inducible NO synthase dimerization. *J Biol Chem* **277**, 47073–47079.

17 Felley-Bosco E, Bender FC, Courjault-Gautier F, Bron C & Quest AFG (2000) Caveolin-1 down-regulates inducible nitric oxide synthase via the proteasome pathway in human colon carcinoma cells. *Proc Natl Acad Sci USA* **97**, 14334–14339.

18 Eaves-Pyles T, Murthy K, Liaudet L, Virag L, Ross G, Soriano FG, Szabo C & Salzman AL (2001) Flagellin, a novel mediator of Salmonella-induced epithelial

activation and systemic inflammation: I kappa B alpha degradation, induction of nitric oxide synthase, induction of proinflammatory mediators, and cardiovascular dysfunction. *J Immunol* **166**, 1248–1260.

19 Zweibaum A, Laburthe M, Grasset E & Louvard D (1991) Use of cultured cell lines in studies of intestinal cell differentiation and function. In *Handbook of Physiology*, (Field M & Frizzell RA, eds), pp. 223–255. American Physiology Society, Bethesda.

20 Vecchini F, Pringault E, Billiar TR, Geller DA, Hausel P & Felley-Bosco E (1997) Decreased activity of inducible nitric oxide synthase type 2 and modulation of the expression of glutathione S-transferase alpha, bcl-2, and metallothioneins during the differentiation of CaCo-2 cells. *Cell Growth Differ* **8**, 261–268.

21 Wheeler MA, Smith SD, Garcia-Cardena G, Nathan CF, Weiss RM & Sessa WC (1997) Bacterial infection induces nitric oxide synthase in human neutrophils. *J Clin Invest* **99**, 110–116.

22 Daniliuc S, Bitterman H, Rahat MA, Kinarty A, Rosenzweig D & Nitza L (2003) Hypoxia inactivates inducible nitric oxide synthase in mouse macrophages by disrupting its interaction with alpha-actinin 4. *J Immunol* **171**, 3225–3232.

23 Ratovitski EA, Alam MR, Quick RA, McMillan A, Bao C, Kozlovsy C, Hand TA, Johnson RC, Mains RE, Eipper BA & Lowenstein CJ (1999) Kalirin inhibition of inducible nitric-oxide synthase. *J Biol Chem* **274**, 993–999.

24 Shenolikar S & Weinman EJ (2001) NHERF: targeting and trafficking membrane proteins. *Am J Physiol Renal Physiol* **280**, F389–F395.

25 Berryman M, Franck Z & Bretscher A (1993) Ezrin is concentrated in the apical microvilli of a wide variety of epithelial cells whereas moesin is found primarily in endothelial cells. *J Cell Sci* **105**, 1025–1043.

26 Sennequier N, Wolan D & Stuehr DJ (1999) Antifungal imidazoles block assembly of inducible NO synthase into an active dimer. *J Biol Chem* **274**, 930–938.

27 Kuncewicz T, Balakrishnan P, Snuggs MB & Kone BC (2001) Specific association of nitric oxide synthase-2 with Rac isoforms in activated murine macrophages. *Am J Physiol* **281**, F326–F336.

28 Darling KEA & Evans TJ (2003) Effects of nitric oxide on Pseudomonas aeruginosa infection of epithelial cells from a human respiratory cell line derived from a patient with cystic fibrosis. *Infect Immun* **71**, 2341–2349.

29 Russwurm M, Wittau N & Koesling D (2001) Guanylyl Cyclase/PSD-95 interaction. Targeting of the nitric oxide-sensitive alpha 2beta 1 guanylyl cyclase to synaptic membranes. *J Biol Chem* **276**, 44647–44652.

30 Mergia E, Russwurm M, Zoidl G & Koesling D (2003) Major occurrence of the new alpha(2)beta(1) isoform of NO-sensitive guanylyl cyclase in brain. *Cell Signal* **15**, 189–195.

31 Huie RE & Padmaja S (1993) The reaction of NO with superoxide. *Free Rad Res Commun* **18**, 195–199.

32 Beckman JS & Koppenol WH (1996) Nitric oxide, superoxide, and peroxynitrite: the good, the bad, and the ugly. *Am J Physiol* **271**, C1424–C1437.

33 Suh Y-A, Arnold RS, Lassegue B, Shi J, Xu X, Sorescu D, Chung AB, Griendin KK & Lambeth JD (1999) Cell transformation by the superoxide-generating oxidase Mox1. *Nature* **401**, 79–82.

34 Banfi B, Maturana A, Jaconi S, Arnaudeau S, Laforge T, Sinha B, Ligeti E, Demaurex N & Krause K-H (2000) A mammalian H^+ channel generated through alternative splicing of the NADPH oxidase homolog NOH-1. *Science* **287**, 138–142.

35 Kawahara T, Kuwano Y, Teshima-Kondo S, Takeya R, Sumimoto H, Kishi K, Tsunawaki S, Hirayama T & Rokutan K (2004) Role of nicotinamide adenine dinucleotide phosphate oxidase 1 in oxidative burst response to toll-like receptor 5 signaling in large intestinal epithelial cells. *J Immunol* **172**, 3051–3058.

36 Kuo PC & Abe KY (1995) Cytokine-mediated production of nitric oxide in isolated rat hepatocytes is dependent on cytochrome P-450III activity. *FEBS Lett* **360**, 10–14.

37 Courjault-Gautier F, Aurora A & Felley-Bosco E (2000) Induction time-course and subcellular distribution of the human inducible nitric oxide synthase in an intestinal cell line: evidence for post-translational regulation. In *The Biology of Nitric Oxide Part 7*, (Moncada S, Gustafsson LE, Wiklund NP & Higgs EA, eds), p. 155. Portland Press, London.

38 Sierro F, Dubois B, Coste A, Kaiserlian D, Kraehenbuhl JP & Sirard JC (2001) Flagellin stimulation of intestinal epithelial cells triggers CCL20-mediated migration of dendritic cells. *Proc Natl Acad Sci USA* **98**, 13722–13727.

39 Geller DA, Lowenstein CJ, Shapiro RA, Nussler AK, Di Silvio M, Wang SC, Nakayama DK, Simmons RL, Snyder SH & Billiar TR (1993) Molecular cloning and expression of inducible nitric oxide synthase from human hepatocytes. *Proc Natl Acad Sci USA* **90**, 3491–3495.

40 Bermeyer HU & Bernt E (1974) Lactate deshydrogenase UV-assay with pyruvate and NADH. In *Methods of Enzymatic Analysis* (Bermeyer HU, ed.), pp. 574–579. Academic Press, New York.

41 Féraille E, Carranza ML, Gonin S, Béguin P, Pedemonte C, Rousselot M, Caverzasio J, Geering K, Martin P-Y & Favre H (1999) Insulin-induced stimulation of Na^+,K^+-ATPase activity in kidney proximal tubule cells depends on phosphorylation of the æ-subunit at Tyr-10. *Mol Biol Cell* **10**, 2847–2859.

42 Glass GA, DeLisle DM, DeTogni P, Gabig TG, Magee BH, Markert M & Babior BM (1986) The

respiratory burst oxidase of human neutrophils. Further studies of the purified enzyme. *J Biol Chem* **261**, 13247–13251.

43 Felley-Bosco E, Ambs S, Lowenstein CJ, Keefer LK & Harris CC (1994) Constitutive expression of inducible nitric oxide synthase in human bronchial epithelial cells induces c-fos and stimulates the cGMP pathway. *Am J Respir Cell Mol Biol* **11**, 159–164.

44 Rumbo M, Sierro F, Debard N, Kraehenbuhl J-P & Finke D (2004) Lymphotoxin α receptor signaling induces the chemokine CCL20 in intestinal epithelium. *Gastroenterology* **127**, 213–223.